

## Subdiffusive exciton motion in systems with heavy-tailed disorder

S. M. Vlaming, V. A. Malyshev, A. Eisfeld, and J. Knoester

Citation: *J. Chem. Phys.* **138**, 214316 (2013); doi: 10.1063/1.4808155

View online: <http://dx.doi.org/10.1063/1.4808155>

View Table of Contents: <http://jcp.aip.org/resource/1/JCPSA6/v138/i21>

Published by the AIP Publishing LLC.

### Additional information on J. Chem. Phys.

Journal Homepage: <http://jcp.aip.org/>

Journal Information: [http://jcp.aip.org/about/about\\_the\\_journal](http://jcp.aip.org/about/about_the_journal)

Top downloads: [http://jcp.aip.org/features/most\\_downloaded](http://jcp.aip.org/features/most_downloaded)

Information for Authors: <http://jcp.aip.org/authors>

## ADVERTISEMENT



**physicstoday**

Comment on any  
*Physics Today* article.

Physics Today / Volume 65 / Issue 7 / July 2012  
Previous Article | Next Article

**Measured energy in Japan**  
David von Seggern  
(dovseg@seismo.unr.edu) University of Nevada  
July 2012, page 10  
DIGITAL OBJECT IDENTIFIER  
<http://dx.doi.org/10.1063/PT.3.1619>

The article by Thorne Lay and Hiroo Kanamori (2012) is an excellent review of the 1964 Chilean earthquake. The authors state that the seismic energy released was approximately five times as much energy as that of a 30-megaton nuclear detonation event—a 30-megaton atmospheric event. The 1964 Chilean earthquake had still more energy by a factor of about 3, or 15 times as much energy as that of a 30-megaton nuclear device. I believe the authors used the relation for seismic energy release rather than total strain energy release. The seismic energy underestimates the total strain energy release by a variable that depends on friction on the fault plane. Accounting for total strain energy release would increase the earthquake energy number by orders of magnitude.

Despite the catastrophic damage potential of nuclear bombs, the forces of nature occasionally unleash much larger energy releases. Although the nuclear bombs are under our control, earthquakes, volcanic eruptions, and extreme weather events are not. However, by judicious preparation and avoidance measures, humans can significantly diminish the damage of natural events.

This article does not have any references.

**Comment on this article**  
By the act of hitting a ball with a bat, one calculates the force energy to deliver the ball to its new location, but one must also take into account that the ball extended its energy to the entire team, which became struck by the ball as its momentum ceased and passed energy to the entire team. Therefore the parameters of the damage extend into the future when the received energy to that pushed upon, later becomes released in a new event. Perhaps calculations of one added that in, while another's calculations did not. E.M.C.  
Written by Edgar McCarvill, 14 July 2012 19:59

## Subdiffusive exciton motion in systems with heavy-tailed disorder

S. M. Vlaming,<sup>1,2,3,a)</sup> V. A. Malyshev,<sup>1</sup> A. Eisfeld,<sup>3</sup> and J. Knoester<sup>1</sup>

<sup>1</sup>Centre for Theoretical Physics and Zernike Institute for Advanced Materials, University of Groningen, Nijenborgh 4, 9747 AG Groningen, The Netherlands

<sup>2</sup>Center for Excitonics and Department of Chemistry, Massachusetts Institute of Technology, 77 Massachusetts Avenue, Cambridge, Massachusetts 02139, USA

<sup>3</sup>Max Planck Institute for Physics of Complex Systems, Nöthnitzer Strasse 38, D-01187 Dresden, Germany

(Received 1 March 2013; accepted 16 May 2013; published online 7 June 2013)

We study the transport of collective excitations (Frenkel excitons) in systems with static disorder in the transition energies, not limiting ourselves to Gaussian transition energy distributions. Instead, we generalize this model to the wider class of Lévy stable distributions, characterized by heavy tails. Phonon-assisted scattering of excitons, localized by the disorder, leads to thermally activated exciton motion. The time evolution of the second moment of the exciton distribution is shown to be sublinear, thus indicating that the exciton dynamics in such systems is not diffusive, but rather subdiffusive instead. The heavier the tail in the transition energy distribution is, the larger are the deviations from the diffusive regime. This from fluctuations of site energies larger than the exciton band width (outliers). We show that the occurrence of subdiffusive transport for heavy-tailed disorder distributions can be understood from the scattering rate distributions, which possess a (second) peak at zero scattering rate. © 2013 AIP Publishing LLC. [<http://dx.doi.org/10.1063/1.4808155>]

### I. INTRODUCTION

Excitons play a major role as energy carriers in a wide variety of both natural and artificial systems, such as photosynthetic complexes,<sup>1–4</sup> conjugated oligomer aggregates,<sup>5</sup> polymers,<sup>6,7</sup> organic dyes embedded in a polymer matrix,<sup>8</sup> molecular aggregates,<sup>9–13</sup> semiconductor quantum wells and wires,<sup>14–16</sup> and organic solar cells.<sup>17</sup> In many such systems, the nature of the exciton motion affects the efficiency and functionality of the system to a large extent. For example, in light harvesting systems and photovoltaic materials, a photon absorbed by the material gives rise to the creation of an exciton. Subsequently, the exciton can diffuse to a reaction center or interface, where charge separation takes place and the energy of the excitation can be harnessed for useful purposes. The exciton needs to be sufficiently mobile to reach the charge separation region within its typical lifetime. Similarly, the functioning of organic light emitting systems is strongly affected by exciton-exciton annihilation which, in turn, is strongly dependent on the motion of excitons.<sup>18–21</sup>

Despite the complex chemical structures that the relevant chromophores typically possess, theoretical approaches based on tight-binding models have been successfully applied to describe the optical properties and excitation dynamics in such systems.<sup>22–26</sup> It has been realized that the effect of the environment that the chromophores are embedded in is crucial in providing an appropriate description of the excitation dynamics.<sup>22,23,27,28</sup> There are a number of commonly used approaches to account for interactions with the environment, also depending on the typical timescale on which environmental changes take place. Changes that are slow compared to the relevant exciton dynamics timescale are often modeled as

static disorder,<sup>29,30</sup> where the host material essentially plays the role of a time independent stochastic potential the exciton moves in. Faster environmental dynamics are referred to as dynamic disorder. The exciton may also couple to vibrational modes when it moves from one molecule to the other. As discussed, e.g., in Ref. 31, such vibrations can be included in the “environment.”

The standard disorder models consider Gaussian or box distributions of the chromophore energies or interchromophore interactions. These distributions may, however, not always be an appropriate choice. This is supported by single molecule studies on chromophores embedded in a glassy host, where it has been shown both experimentally and theoretically that the absorption lines are heavy-tailed.<sup>32–35</sup> Such heavy-tailed distributions are known as Lévy stable distributions.<sup>36</sup> During the past 20 years, it has been recognized that Lévy statistics are relevant in a variety of subfields of the natural sciences, ranging from statistical physics to optics, plasma physics, and condensed matter physics.<sup>37–45</sup>

In this paper, we study the transport properties of a one-dimensional Frenkel exciton chain of  $N$  coupled chromophores with transition energies randomly taken from a symmetric Lévy stable distribution. As has been shown in our previous publication,<sup>37</sup> this choice can lead to significant qualitative changes in the absorption spectra (exchange broadening and blue shift of the maximum instead of exchange narrowing and red shift found for Gaussian randomness) as well as on the localization properties of the model (additional structure in the localization length distribution). Many of these effects originate from the heavy tails of the Lévy stable distribution, resulting in frequently occurring outliers, i.e., large fluctuations in chromophore transition energies. The latter produce energy barriers, leading to weakly coupled segments in the chain that are capped by these

<sup>a)</sup>Electronic mail: vlaming@pks.mpg.de

barriers, and one expects that this slows down the transport. Similar questions arise in molecular motion in systems with material barriers (membranes) in porous media, composites, and biological tissues.<sup>46</sup>

We scrutinize the low-temperature exciton dynamics in such Lévy disordered systems by extending the methodology previously put forth in Refs. 22. The excitons are taken to be weakly coupled to environmental phonon modes. This coupling essentially leads to the scattering of excitons on phonon modes. We are mainly interested in the low temperature exciton dynamics, where scattering on long wavelength acoustic phonons is the dominant transport mechanism. For delocalized excitations, the exciton-phonon coupling is strongly reduced, supporting the validity of the perturbational approach used here.<sup>22</sup> The scattering events on the aforementioned acoustic phonon modes provide an inhomogeneous hopping mechanism between the various exciton states. For the molecular J-aggregates that we will consider here, the relevant exciton states for absorption and thermally activated exciton transport have an energy close to the bare exciton lower band edge. Of particular relevance are the localized states that reside in the tail of the exciton density of states, just below the exciton band edge, the so-called Lifshits tail.<sup>47</sup>

In this work, we show numerically that the exciton motion in a heavy-tailed disordered system is generally not diffusive, but subdiffusive instead. This is done by calculating the time evolution of the second moment of the exciton wave packet's position. We find a sublinear time dependence of the second moment, indicating a subdiffusive exciton motion. We show that the subdiffusive transport is linked to the increased occurrence of outlier-induced barriers. This is confirmed by analyzing the changes in the relevant scattering rate and overlap distributions, where heavy-tailed disorder distributions are shown to lead to additional peaks that are directly related to the presence of these barriers.

The paper is organized as follows. The basic Frenkel exciton Hamiltonian and the concept of localization is introduced in Sec. II A. Then, we proceed with discussing how to model the excitation dynamics in Sec. II B. The numerical results are presented in Sec. III. First, we present the results on the exciton motion in Sec. III A, which are analyzed and put into a proper theoretical perspective in Sec. III B. Finally, we summarize and conclude in Sec. IV. Details on the master equation used for the excitation propagation can be found in the Appendix.

## II. THEORETICAL FRAMEWORK

### A. Hamiltonian and localization

We consider the single-exciton manifold of a one-dimensional Frenkel exciton chain (sites are labeled by  $n = 1, \dots, N$ ), described by the Hamiltonian<sup>48–50</sup>

$$H = \sum_n E_n b_n^\dagger b_n + \sum_{n,m \neq n} J_{nm} b_n^\dagger b_m. \quad (1)$$

Here,  $b_n^\dagger$  ( $b_n$ ) is the creation (annihilation) operator of an excitation at site  $n$  and  $J_{nm}$  is the interaction between sites  $n$  and  $m$ , which we will take as either a nearest-neighbor interaction

$J_{nm} = -J(\delta_{m,n-1} + \delta_{m,n+1})$ , or as a dipole-dipole interaction,  $J_{nm} = -J/|n-m|^3$ , where in both cases, we consider  $J > 0$ . We consider the case of negative coupling  $J_{nm}$  which corresponds to the important class of J-aggregates, where the absorption is red shifted with respect to that of a single monomer. For positive  $J_{nm}$ , we would find very similar results. We will comment on this extension at the appropriate places. We consider uncorrelated diagonal disorder,<sup>37</sup> that is, the molecular transition energies  $E_n$  are independently taken from a certain distribution. In this work, we focus on the symmetric (Lévy) stable distributions,

$$P(E) = \frac{1}{2\pi} \int_{-\infty}^{\infty} dt e^{iEt} \exp(-|\sigma t|^\alpha), \quad (2)$$

where the scale parameter  $\sigma$  determines the width of the distribution and the stability index  $0 < \alpha \leq 2$  fixes the asymptotic behavior. Generally, a smaller value of  $\alpha$  implies more weight in the tails of the distribution. Note that, except for  $\alpha = 2$  (Gaussian disorder), the second and higher order moments of the Lévy stable distribution diverge. Thus the Gaussian central limit theorem (an infinite sum of independent random variables which have finite variance converges against a Gaussian distribution) is not applicable. However, for each Lévy stable distribution there exists a similar central limit theorem. As shown by, e.g., Gnedenko and Kolmogorov, the sum of identical random variables with power-law tail distributions decreasing as  $|x|^{-\alpha-1}$  where  $0 < \alpha < 2$  (and therefore having infinite variance) will tend to a stable distribution with an index of stability  $\alpha$  as the number of variables grows.<sup>36</sup> An important property of the considered Lévy stable distributions is that if the  $x_n$  are distributed according to Eq. (2), then its average  $y = \frac{1}{M} \sum_{n=1}^M x_n$  is distributed according to a Lévy stable distribution with the same value of  $\alpha$ , but a renormalized width,

$$\sigma^* = \sigma M^{(1-\alpha)/\alpha}. \quad (3)$$

This property is referred to as the stability of the distribution.

We are interested in transport of a single excitation along the aggregate. Thus we expand the Hamiltonian Eq. (1) with respect to one-exciton states  $|n\rangle$ , where site  $n$  is electronically excited and all other sites are in their ground state. An arbitrary state can be expanded in this basis according to

$$|s\rangle = \sum_{n=1}^N c_{sn} |n\rangle, \quad (s = 1, \dots, N). \quad (4)$$

In the following, we will always use the notation  $|s\rangle$  to refer to an eigenstate of the Hamiltonian (1) in the subspace spanned by the states  $|n\rangle$ , which for a given realization can simply be found by numerical diagonalization of the Hamiltonian matrix. The localization length of such an exciton state can be defined in various ways; we employ the Participation Number (PN),<sup>51–53</sup> defined as  $L_s = (\sum_{n=1}^N |c_{sn}|^4)^{-1}$ . It can be straightforwardly checked that this definition gives the expected result in the limits of completely delocalized ( $c_{sn} = 1/\sqrt{N}$ , for periodic boundary conditions) and completely localized ( $c_{sn} = \delta_{n,n_0}$ ) states.

As has been shown in Ref. 37, the localization behavior and the resulting optical properties for such

heavy-tailed disorder ( $\alpha < 2$ ) differ considerably from conventional localization, where states localize in the effective potential wells produced by the typical fluctuations of the transition energies.<sup>47</sup> First of all, the exciton absorption peak need not to be narrower than the monomer peak as the conventional exchange narrowing effect predicts,<sup>54</sup> but the opposite effect of exchange broadening may occur. In fact, already for Lorentzian disorder ( $\alpha = 1$ ) it is expected that exchange narrowing is absent.<sup>55,56</sup> Second, the scaling of the localization length with disorder will change considerably, while in addition the universality of the localization length distribution will break down.

Of particular relevance in the present case is that heavy-tailed disorder distributions also support the frequent occurrence of outliers, which are molecules whose transition energy occurs in the tails of the distribution outside of the exciton band. Note that outliers can in principle occur for Gaussian disorder as well, in particular when the width of the distribution is of a comparable magnitude to the exciton bandwidth; however, more heavy-tailed distributions already support non-negligible amounts of outliers for considerably smaller disorder values  $\sigma$ . These outliers, which we here define as molecules  $n$  with  $|E_n| > 2.5J$ , i.e., with an energy outside of the bare exciton band, typically do not coherently share their excitation with their neighbors to any appreciable extent, due to the large transition energy difference. However, when the molecular excitation energy is not too far below the exciton band edge ( $E = -2J$  for nearest neighbor interactions,  $E = -2.4J$  for dipole-dipole interactions), a local low energy exciton state may be supported that still has an appreciable overlap with other exciton states. For details on these topics, we refer to Refs. 37 and 55. Most relevant for the study of excitation energy transport is the change in hidden structure, that is, the structure of the wave functions near the exciton band edge.<sup>57,58</sup> A typical realization is shown in Fig. 1, and it

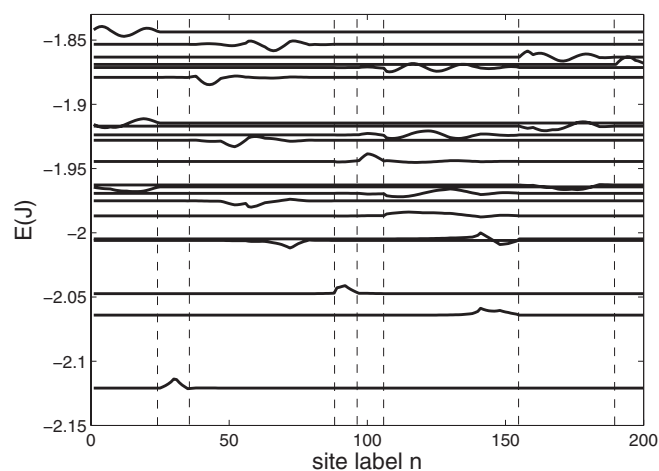


FIG. 1. Typical realization of exciton wave functions for a Lévy disordered chain ( $\alpha = 1/2$ ,  $\sigma = 0.1J$ ) around the exciton band edge. The vertical offset of the wave functions corresponds to the exciton energy, while the actual amplitude is not related to an energy but illustrates the shape of the wave functions. The vertical lines correspond to molecules with either a very high or a very low energy ( $|E_n| > 2.5J$ ), and these outliers effectively divide the chain into a set of weakly coupled, shorter subchains. Note that typically the wave functions hardly extend across these segment boundaries.

is clear that segmentation takes place. Each localization segment is bounded by two outliers, effectively subdividing the chain into a set of weakly coupled subchains. The occurrence of these segment boundaries is expected to strongly reduce the exciton motion, and as will be shown in Sec. III, subdiffusive transport is to be expected.

## B. Exciton dynamics

The interactions with the environment make it possible for the exciton to scatter between states. On the one hand this gives rise to exciton relaxation, while on the other hand it also supports the movement of the excitation within the supramolecular system. We allow for scattering of the excitons on environmental acoustic phonon modes, and employ the Pauli master equation approach to follow the time evolution of the exciton populations (see, e.g., Refs. 22, 23, 48, and 59).

We describe the time evolution of the populations of the eigenstates  $|s\rangle$  by the Pauli master equation

$$\dot{P}_s(t) = \sum_{s'} [W_{ss'} P_{s'}(t) - W_{s's} P_s(t)], \quad (5)$$

where  $W_{ss'}$  is the scattering rate from exciton state  $|s'\rangle$  to  $|s\rangle$ . The details of this formalism, including the explicit expressions for the scattering rates, are given in the Appendix. Here, we only note that the scattering rates  $W_{ss'}$  are proportional to an overlap factor between the states  $|s'\rangle$  to  $|s\rangle$ .

We are primarily interested in quantifying how the excitation packet propagates spatially. As detailed in the Appendix, due to symmetry, the disorder-averaged displacement vanishes, so we choose to use the second moment of the excitation to characterize the type of transport that occurs. For diffusive behavior, the second moment should evolve linearly in time; deviations from this behavior is thus direct evidence of non-diffusive transport. For an excitation that is initially localized on site  $n_0$ , we define the second moment as

$$\begin{aligned} \langle n^{(2)}(t) \rangle &= \sum_n p_n(t) (n - n_0)^2 \\ &= \sum_n \sum_s P_s(t) |c_{sn}|^2 (n - n_0)^2, \end{aligned} \quad (6)$$

where  $P_s$  is the population of exciton state  $s$ , and  $p_n$  is the population of monomer  $n$  in the site basis.

As stated before, the second moment is often used to characterize the type of transport. Ballistic transport implies that the second moment evolves quadratically in time, diffusive motion corresponds to a second moment that evolves linearly in time, while subdiffusive transport shows a second moment that increases even more slowly.<sup>38,60–62</sup> For diffusive transport, the time dependence of the second moment can be written as  $\langle n^{(2)}(t) \rangle = 2Dt$ , where the proportionality constant  $D$  is called the diffusion coefficient.

## III. NUMERICAL RESULTS

In this section, we provide the results of our numerical calculations and put them in a theoretical perspective. First of

all, we introduce and motivate the relevant initial conditions, and define the parameter values that are used in the model calculations. Then, in Sec. III A, we present the time evolution of the second moment of the excitation, for various parameter values and for both nearest-neighbor and dipole-dipole interactions, where we show that subdiffusive behavior occurs. Finally, in Sec. III B, we argue that the subdiffusive behavior is due to the introduction of segment boundaries and traps that act as blockades for the excitation movement. This is substantiated by considering the distributions of scattering rates and overlaps, where heavy-tailed disorder distributions are shown to lead to the emergence of a two-peaked structure in the scattering rate and overlap distributions. The additional peak corresponds to exciton states that couple weakly to its neighbors, which effectively impede the exciton transport.

In our numerical simulations, we follow the procedure outlined in Sec. II B and detailed in the Appendix, and calculate the time evolution of the averaged mean square displacement (Eq. (6)). Experimentally, an excitation is usually created by the absorption of light; the exciton states that do so most strongly are those around the exciton band edge that have no nodes, since for such exciton states all molecules contribute coherently to the absorption if all transition dipoles of the monomers are assumed to be parallel and identical. Therefore, in our simulations for each realization of the disorder, we initially populate the exciton state that satisfies the following requirements:

- it is an *s*-like state (i.e., without nodes), which we determine by the criterion<sup>63</sup>

$$\left| \sum_n c_{sn} |c_{sn}| \right| \geq C_0. \quad (7)$$

We take  $C_0 = 0.9$  in our simulations to select states where a sufficiently large fraction of the molecules absorb in phase.

- it is sufficiently delocalized, i.e., it is not an outlier (in practice, we require a minimum value of the Participation Number,  $L_s > 3$ .) Again, this is done to select an exciton state with sufficient oscillator strength to be relevant for absorption, and which lies around the exciton band edge.
- we choose the spatially most central exciton state that satisfies the above requirements, in order to minimize the occurrence of finite size effects.

The system is then allowed to evolve in time and we average over typically a few thousand up to ten thousand realizations. We do these calculations for both nearest-neighbor (NN) and long-range dipole-dipole (LR) interactions. In the simulations below, we consider chains of length  $N = 500$ . This is sufficiently large to avoid finite size effects for the parameters considered. The nearest-neighbor interaction  $J$  is taken as the unit of energy. Unless noted otherwise, the temperature is  $0.116J$ , corresponding to a temperature of 100 K in case of nearest neighbor interactions of a strength appropriate for pseudoisocyanine (PIC) aggregates, where  $J \approx 600 \text{ cm}^{-1}$ .<sup>64,65</sup> We choose a scattering amplitude  $W^{(0)} = 10J$ , which is of the correct order of magnitude for PIC

aggregates.<sup>23</sup> Let us briefly comment on differences when one uses a coupling between the sites which is positive. This corresponds to the case of so called H-aggregates, where the absorption is shifted to the blue.<sup>66</sup> Then, in contrast to the present situation, the initial state would be at the top of the exciton band and the initial dynamics would be dominated by relaxation to the bottom of the band. After that initial stage, a very similar type of dynamics sets in as the one that will be described in the remainder of this work.

Note that, while the scattering amplitude  $W^{(0)}$  is related to the strength of the exciton-phonon coupling, in addition it involves a large number of other constants and prefactors.<sup>22,23</sup> The resulting value of  $W^{(0)} = 10J$  is much larger than the bare exciton-phonon coupling strength. The presence of energetic and overlap factors in Eq. (A2) reduces the actual exciton scattering rates  $W_{s,s'}$  to values far lower than  $W^{(0)}$ . Finally, we use a cut-off frequency in the spectral density, which is in the order of the interaction  $J$ . This guarantees that there are phonon modes available with frequencies that correspond to energy differences between the exciton states. Specifically, in the following we use  $\omega_c = J/2$ .

## A. Exciton motion

In most cases that we have studied, the time evolution of the second moment can be well fitted by a power law,  $\langle n^{(2)} \rangle \propto t^\delta$ , with an exponent  $\delta < 1$  corresponding to subdiffusive behavior. Since the initial state has a small non-zero second moment as well, we have also fitted the time evolution of the second moment by a power law with offset,  $\langle n^{(2)} \rangle = at^\delta + b$ . Typically, however, this leads to similar values for the fit exponent  $\delta$ , while only marginally improving the quality of the fit. We will therefore proceed with using the simple power law  $\langle n^{(2)} \rangle \propto t^\delta$ .

Typical examples, for  $\alpha = 3/2$  and  $\alpha = 1/2$ , are shown in Fig. 2. Generally, the more heavy-tailed a distribution becomes, the larger will be the deviation from diffusive behavior ( $\delta = 1$ ). As we will discuss in more detail in Sec. III B, this is related to the increased occurrence of outliers, whose corresponding exciton states have a small overlap with its neighbors and which as a result provide barriers for the excitation transport. In addition, there is also an increase in exciton states centered around sites with an excitation energy in or around the Lifshits tail, such that these states still have a considerable overlap with their neighbors but lie sufficiently deep into the Lifshits tail to act as traps. In such cases, scattering into such a local low energy exciton state occurs at considerably higher rates than scattering out of it, thereby reducing the exciton motion. It is observed that even Gaussian disorder seems to produce slightly subdiffusive behavior at long times. This is most likely due to the fact that the likelihood of outliers occurring is small but non-vanishing, and the occurrence of disorder still leads to the introduction of local low energy states that act as traps or barriers. Generally, an increase in the weight in the tails (i.e., smaller  $\alpha$  and/or larger  $\sigma$ ) of the disorder distribution leads to stronger subdiffusive behavior.

While the time dependence of the expectation value of the second moment can generally be well fit by a power law,

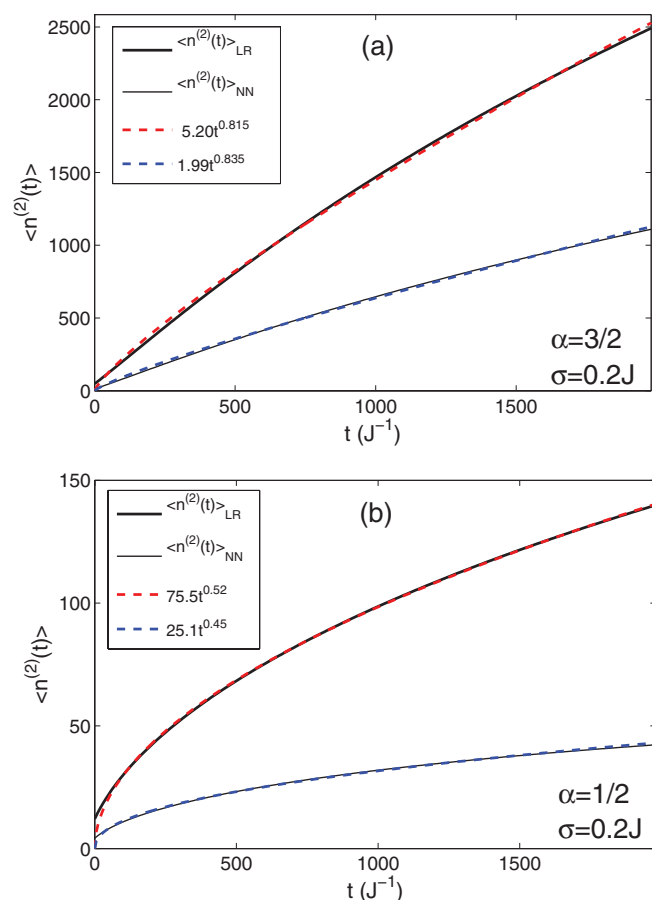


FIG. 2. Time evolution of the second moment  $\langle n^{(2)}(t) \rangle$  of the excitation wave packet calculated for different parameter values and interactions (long-range interactions: thick solid, nearest-neighbor interactions: thin solid), and corresponding power law fits (dashed lines). (a)  $\alpha = 3/2$ ,  $\sigma = 0.2J$ , with power law fits  $\langle n^{(2)}(t) \rangle_{LR} = 5.20t^{0.815}$  (red dashed line), and  $\langle n^{(2)}(t) \rangle_{NN} = 1.99t^{0.835}$  (blue dashed line), (b)  $\alpha = 1/2$ ,  $\sigma = 0.2J$ , with power law fits  $\langle n^{(2)}(t) \rangle_{LR} = 75.5t^{0.52}$  (red dashed line), and  $\langle n^{(2)}(t) \rangle_{NN} = 25.1t^{0.45}$  (blue dashed line).

it is observed that typically the actual expectation value of the second moment increases slightly slower than the best fit power law. This introduces some ambiguity into what the best fit is, as this depends on the time interval considered: the corresponding exponent can change by a few percent. We choose to consider the same time interval in all simulations.

The results reported here do not qualitatively change under the inclusion of long-range dipole-dipole interactions, even though the overall exciton motion does show a considerable quantitative difference. As shown in Fig. 2, subdiffusion is observed to occur for long-range interactions as well. While the degree of subdiffusion, as defined by the exponent  $\delta$  in the time evolution of the second moment, may also differ to a small extent, it is typically of a comparable magnitude. The most striking quantitative difference is in the overall migration rate: typically, long-range interactions allow for faster transport of the excitation by a factor of 2–3. This is most likely due to the fact that long-range interactions allow for a next-nearest-neighbor coupling between molecules on different sides of segment boundaries. A small difference in the exciton transport exponent  $\delta$  between nearest-neighbor and

long-range interactions may occur, but to a reasonable approximation, the quotient of the two second moments is approximately constant in time except for short times.

The time in Fig. 2 is expressed in units of  $J^{-1}$  in order to facilitate application of our results to different physical systems. As mentioned in Sec. III, for a molecular aggregate such as PIC, we have  $J \approx 600 \text{ cm}^{-1}$ , so that the time unit  $J^{-1}$  corresponds to  $1J^{-1} \equiv 1/18 \text{ ps}$ . The total timescale of plots such as Fig. 2 thus corresponds to approximately 100 ps. This is of the same order of magnitude as typical fluorescence decay times for molecular aggregates, and therefore the relevant timescale for the exciton dynamics in these systems.<sup>22,52,64,67–69</sup>

## B. Subdiffusive transport: Theoretical background

From the numerical calculation of the time evolution of the excitation, it is difficult to get an understanding of the underlying physical processes. From considering simpler quantities, it turns out to be possible to qualitatively understand the observed occurrence of subdiffusion.

To make a connection to previously studied diffusion models, it is useful to consider scattering rates that are transformed back to the site basis, which gives effective scattering rates  $\tilde{W}_{nn'}$  from site  $n'$  to site  $n$ ,

$$\tilde{W}_{nn'} = \sum_{s,s'} |c_{sn}|^2 |c_{s'n'}|^2 W_{ss'}. \quad (8)$$

We denote the distribution of scattering rates over a distance  $m$  by  $P(\tilde{W}_m)$  with  $\tilde{W}_m = \tilde{W}_{n,n+m}$ , i.e., we include all possible values of the index  $n$  for which  $\tilde{W}_{n,n+m}$  is defined. It is insightful to consider the distribution of nearest-neighbor scattering magnitudes  $\tilde{W}_{n,n+1}$ , which we will simply denote by  $W_1$ . The distributions are normalized to unity area. For Gaussian disorder ( $\alpha = 2$ ), the distribution consists of one single peak, as shown in Fig. 3. In contrast, for more heavy-tailed distributions such as in Fig. 4, it shows a clear bimodal shape. The first mode, a sharp peak as  $W_1 \rightarrow 0$ , is numerically found to correspond to scattering events involving an initial and

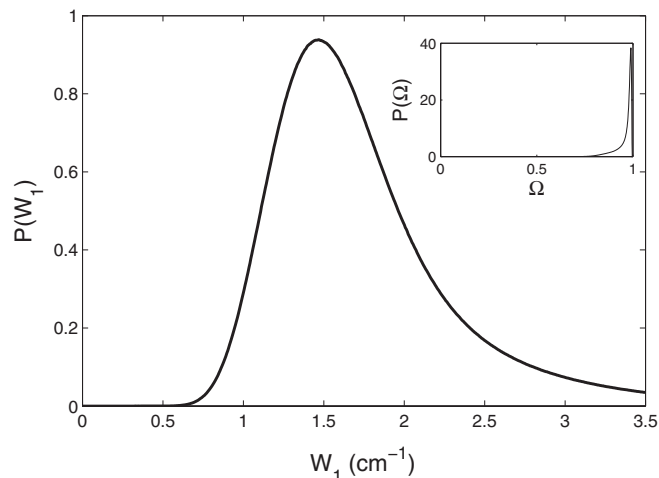


FIG. 3. Distribution of scattering rates  $W_1$  for  $\alpha = 2$ ,  $\sigma = 0.2J$ , and the corresponding overlap distribution in the inset. For clarity, only the distributions for long-range interactions are shown; the distributions for nearest-neighbor interactions are very similar. There is no low- $W_1$  peak visible.

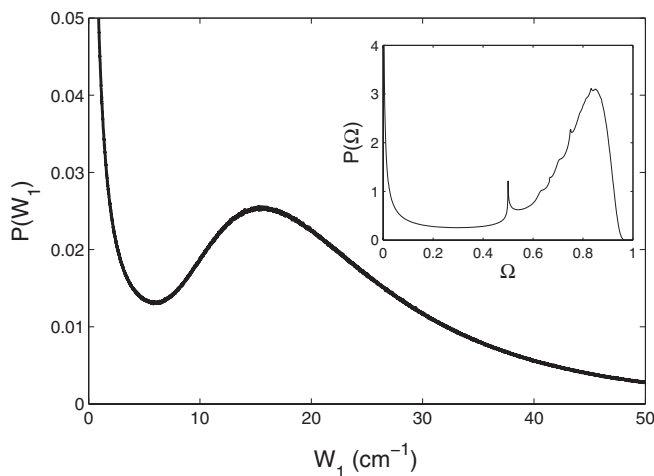


FIG. 4. Distribution of scattering rates  $W_1$  for  $\alpha = 1/2$ ,  $\sigma = 0.2J$ , and the corresponding overlap distribution in the inset. For clarity, only the distributions for long-range interactions are shown; the distributions for nearest-neighbor interactions are very similar. Note the clear bimodal shape: one peak at low  $W_1$  (at low  $\Omega$ ), and a second peak similar to the one obtained for Gaussian disorder (see Fig. 3). The overlap distribution shows additional features, which are explained in the main text.

final site with widely different energies; typically outliers are involved. The second mode is a typical distribution of scattering rates for a system without outliers, and corresponds to intrasegment scattering – analogous to the distribution in Fig. 3. Naturally, the relative size of the two contributions depends on the values of  $\alpha$  and  $\sigma$  that characterize the disorder distribution. Typically, smaller  $\alpha$  and larger  $\sigma$  lead to an increase in outliers and therefore to an increase in importance of the small- $W_1$  peak. This is analyzed quantitatively below.

It is straightforwardly confirmed that this bimodal shape is a localization-induced effect. To see this, let us consider the distribution of the overlap factors, i.e., in the form wherein the overlap also enters the scattering rate Eq. (A2),

$$\Omega_{ss'} = \sum_{s'} \sum_n |c_{sn}|^2 |c_{s'n}|^2. \quad (9)$$

Note that the overlap  $\Omega_{ss'} = \sum_n |c_{sn}|^2 |c_{s'n}|^2$  between states  $s$  and  $s'$  that are localized in different parts of the system is practically zero, an effect that is also present for Gaussian disorder. However, we want to make a distinction between, on the one hand, exciton states that have practically no overlap with any other exciton state, and on the other hand exciton states that do overlap with some (but not necessarily all) other exciton states. Therefore, in Eq. (9), we include a sum over all other exciton states  $s'$  to eliminate the irrelevant practically zero-valued overlap factors with non-adjacent exciton states. This leads to overlap distributions that show a bimodal shape as well, i.e., there are states that hardly overlap with any of its neighbors, and states that do have an overlap with some other exciton states. In the insets of Figs. 3 and 4, the overlap distributions are shown for the cases  $\alpha = 2$  and  $\alpha = 1/2$ , respectively. A comparison of the scattering rate distributions in Figs. 3 and 4 and the corresponding overlap distributions in their insets show that both consist of two main peaks, including one peak at zero scattering rate (zero over-

lap). The energy-dependent prefactors in the scattering rates, such as the spectral density and the thermal phonon occupations, cause a weighing of the various overlap contributions, modifying the details of the distribution but keeping its general bimodal shape intact.

Additional structure can be observed in the overlap distribution for  $\alpha = 1/2$  (e.g., the inset of Fig. 4), consisting of a peak at  $\Omega = 1/2$  and a series of small shoulders at larger values of  $\Omega$ . The peak at  $\Omega = 1/2$  originates from the occurrence of segments that behave effectively as dimers, that is, two neighboring sites whose transition energies happen to have a similar value, while this value is very different from the transition energies of any other neighboring sites. Then, this dimer is approximately decoupled from the rest of the system, and it is straightforwardly shown that such dimer states produce overlap factors of  $\Omega \approx 1/2$ . The small features at larger values of  $\Omega$  correspond, analogously, to effective segments of length three, four, and so on.

While the nearest-neighbor scattering rates  $W_1$  allow for an understanding of the origin of subdiffusive behavior in these systems, it is instructive to see how  $P(\tilde{W}_m)$  evolves with increasing  $m$ . First of all, for more heavy-tailed distributions, the average scattering rate decays with  $m$ , signifying that scatterings over increasingly large distances become less important. This supports our focus on the nearest-neighbor scattering rates. For disorder distributions closer to Gaussian disorder, the average scattering rate might actually initially increase with  $m$ , and peak at some value of  $m > 1$ . This is also reflected in the position of the peak of the second mode, which for increasing  $m$  may first shift to higher values of  $W$ , but will eventually shift towards smaller values of  $W$  as the scattering rates for larger displacements become increasingly small. In addition, while the general bimodal shape is also present for displacements  $m > 1$ , the shape of the distribution does change with increasing displacement  $m$  with the low- $W$  mode obtaining a larger weight at the cost of the intrasegment scattering mode. This is a direct consequence of the increased likelihood of finding outliers and trap states within the scattering distance  $m$ . How quickly the shape changes with increasing disorder strength  $\sigma$  depends strongly on the localization length, i.e., on how likely it is that an increase of the scattering distance leads to encountering an additional outlier.

We will now argue that the bimodal distribution of scattering rates  $P(W_1)$  observed above leads to subdiffusive behavior. It is well known<sup>70,71</sup> that diffusion of a point particle in a chain with randomly distributed nearest-neighbor scattering rates  $W_1$  is diffusive if the expectation value of  $W_1^{-1}$  is finite. However, when the expectation value of  $W_1^{-1}$  diverges, subdiffusive behavior is expected. In particular, previous studies<sup>70,71</sup> have analytically shown that scattering rate distributions of the form  $P(W_1) \propto W_1^{-\beta}$  will lead to long-time subdiffusive behavior. This behavior is related to the results of Scher and Montroll,<sup>72</sup> where the carrier motion in various materials is modeled as a random walk with a long-time tail in the hopping time distribution, showing that such a random walk yields subdiffusive behavior. Since the hopping times are basically the inverses of the scattering rates  $W_1$ , a peak for small  $W_1$  in the scattering rate distribution corresponds to a

tail for large hopping times in the corresponding hopping time distribution. This confirms that indeed our bimodal distribution leads to subdiffusion.

A relevant quantity for understanding to what degree the excitation transport becomes subdiffusive, is the relative weight of the intersegment scattering mode (ISSM), which we define as

$$\Lambda^{W_1} = \frac{\left[ \int_0^{W_1^{\min}} P(W_1) dW_1 \right]}{\int_0^\infty P(W_1) dW_1}. \quad (10)$$

Here, the ISSM is defined as the part of the distribution from  $W_1 = 0$  up to the local minimum separating the two modes, where we denote the corresponding value of  $W_1$  by  $W_1^{\min}$ .

The quantity  $\Lambda^{W_1}$  can be interpreted as the fraction of sites that are only weakly coupled to their neighbors. We can define a similar quantity for the overlap distributions  $p(\Omega)$ , i.e., the distribution of  $\Omega_s$  for all  $s$ , where analogously to the scattering rate distribution we define  $\Omega_{\min}$  as the value of  $\Omega$  corresponding to the minimum between the two modes,

$$\Lambda^\Omega = \frac{\left[ \int_0^{\Omega_{\min}} p(\Omega) d\Omega \right]}{\int_0^\infty p(\Omega) d\Omega}. \quad (11)$$

Figure 5 shows how  $\Lambda^{W_1}$  and  $\Lambda^\Omega$  depend on disorder, for various values of  $\alpha$ . For any value of  $\alpha$ , both  $\Lambda^{W_1}$  and  $\Lambda^\Omega$  increase as a power law  $\Lambda = a\sigma^\gamma$  with the disorder. For the sake of clarity, Fig. 5 only shows the results for long-range interactions; the results for nearest-neighbor interactions are quite similar. It should be noted that all  $\Lambda$ 's vanish for Gaussian disorder,  $\alpha = 2$  with  $\sigma \lesssim 2J$ . For the heavy-tailed distributions shown in Fig. 5, excellent power law fits can be made for  $\Lambda = a\sigma^\gamma$ , in all cases yielding an exponent  $\gamma \approx \alpha$ . Specifically, in the order presented in the legend of Fig. 5, we

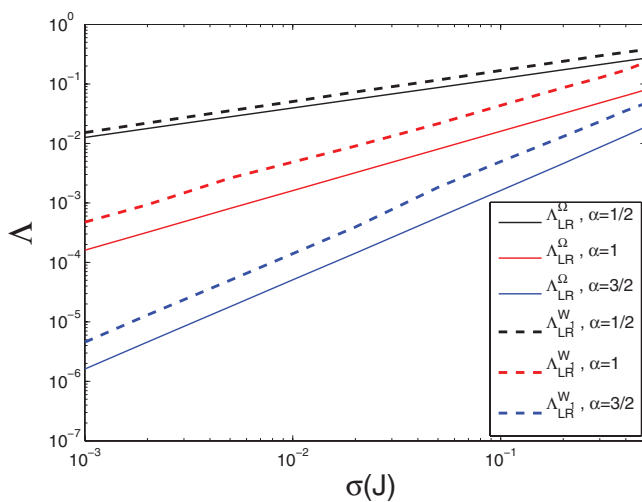


FIG. 5. Disorder dependence of the relative weight of the first mode in, respectively, the scattering rate distributions and the overlap distributions for long-range interactions, for the values  $\alpha = 1/2$ ,  $\alpha = 1$ , and  $\alpha = 3/2$ . The relative weights for nearest-neighbor interactions are nearly identical to those for long-range interactions, and are not shown here for clarity. Note that, for a fixed value of  $\alpha$ , all these measures scale (almost) identically with the disorder strength and only differ in an overall prefactor in the scaling power law.

obtain the following fit exponents:  $\gamma_{1/2}^\Omega = 0.49 \pm 0.01$ ,  $\gamma_1^\Omega = 1.00 \pm 0.01$ ,  $\gamma_{3/2}^\Omega = 1.55 \pm 0.04$ ,  $\gamma_{1/2}^W = 0.51 \pm 0.01$ ,  $\gamma_1^W = 0.99 \pm 0.01$ , and  $\gamma_{3/2}^W = 1.41 \pm 0.06$ . It is striking that all exponents  $\gamma$  are almost equal for any given value of  $\alpha$ , independent of whether we use nearest-neighbor rates or overlaps, or whether we use nearest-neighbor or long-range dipole-dipole interactions. The difference is purely in the prefactor of the scaling relation. This suggests that the distribution of localization segments and their overlap properties, as dictated by the disorder distribution, determine to what extent the distributions are separated into a weakly scattering (low-overlap) intersegment mode and a strongly scattering (high-overlap) intrasegment mode; the details of the intermolecular interactions or energy-dependent prefactors are relatively unimportant here.

The fact that the scaling exponent obeys  $\gamma \approx \alpha$  can be understood quantitatively. We have argued before that the peaks at small scattering rates (small overlaps) correspond to barriers in the excitation transport, related to outliers in transition energy. These barriers then correspond to sites sufficiently deep in the tail of the Lévy stable distribution, where one can approximate the stable distribution  $P(E)$  by<sup>73</sup>

$$P(E) \sim \frac{\sigma^\alpha \sin(\pi\alpha/2) \Gamma(\alpha + 1)}{\pi |E|^{1+\alpha}}. \quad (12)$$

The weight  $Y$  of the tails beyond some energy  $E_0$ , i.e., the area of the distribution with  $|E| > E_0$ , is obtained from a straightforward integration of Eq. (12), yielding

$$Y = \frac{2 \sin(\pi\alpha/2) \Gamma(\alpha + 1)}{\pi \alpha E_0^\alpha} \sigma^\alpha \propto \sigma^\alpha. \quad (13)$$

The tail weight  $Y$  thus shows exactly the same scaling behavior with disorder  $\sigma$  as was previously observed for the relative weight  $\Lambda^{W_1}$  ( $\Lambda^\Omega$ ) of the small scattering rate (overlap) peak, confirming our assignment of these peaks to barriers corresponding to outliers.

For increasing disorder  $\sigma$ , the relative weight of the low-overlap (or low scattering rate) mode  $\Lambda$  increases and the subdiffusive exponent  $\delta$  decreases. It is thus not surprising that both quantities are anti-correlated for fixed values of the stability index  $\alpha$ . It is, however, not possible to obtain a general one-to-one relation between the two: while the two quantities are anti-correlated for fixed  $\alpha$ , this no longer holds when combining these quantities obtained for different values of  $\alpha$ .

## IV. CONCLUSIONS

The dynamics of excitations in disordered systems are shown to depend crucially on the type of disorder involved. The considerable changes in localization behavior that have previously been uncovered to occur for disorder distributions with heavy tails<sup>37</sup> are reflected in the exciton motion as well. In particular, molecules with transition energies in the tails of the distribution will coherently share their excitation with their neighbors to a small extent, effectively acting as segment boundaries separating the system into weakly coupled subchains of variable length. This change in the wave function structure near the lower exciton band edge has consequences for the exciton transport in such systems as well. To

this end, we study the time evolution of the second moment of an excitation in disordered systems, where the molecular excitation energies are represented by uncorrelated stochastic variables taken from a symmetric Lévy stable distribution. In such systems, diffusive behavior will in general not occur, as the second moment does not increase linearly in time, but as a power law  $\langle n^{(2)}(t) \rangle \propto t^\delta$  with an exponent  $\delta < 1$ . The disorder-induced segmentation of the exciton wave functions and the increased occurrence of deep-lying low energy exciton states (outliers) inhibits the exciton motion and leads to subdiffusive behavior instead.

Generally, the more weight is in the tails of the disorder distribution, the stronger the deviation from diffusive behavior is, as is indicated by a decrease in the exponent  $\delta$ . Calculation of the distribution in scattering rates and overlaps makes this behavior more insightful, as these show the appearance of an additional peak at small scattering rates (overlaps), reflecting the presence of barriers in the excitation transport. The relative weight  $\Lambda$  of this additional peak scales with disorder as a power law  $\Lambda \propto \sigma^\alpha$ , independent of the choice of interaction and independent of whether we consider scattering rates or overlaps. This scaling behavior is identical to the scaling of the tail weight of the original Lévy distribution, indicating that the emergence of the small scattering rate and small overlap peaks is indeed caused by an increased frequency of outliers.

However, while the disorder strength  $\sigma$ , the time evolution exponent  $\delta$  and the relative weight of the small-scattering (or small-overlap) mode  $\Lambda$  can all be correlated with each other for a fixed type of Lévy stable distribution (i.e., for a fixed  $\alpha$ ), no one-on-one relation between the various studied quantities has been found that holds for all  $\alpha$ . Finally, the excitation transport has been studied for both nearest-neighbor and long-range interactions. The degree of subdiffusion, as defined by the time evolution exponent  $\delta$ , does not differ appreciably, but there is an overall increase in exciton migration for long-range interactions. This finds its origin in an increase in overlap between states on different localization segments.

## ACKNOWLEDGMENTS

The authors would like to thank Robert J. Silbey for useful discussions, and Sebastian Möbius for assistance with numerical simulations. S.M.V. acknowledges support of this work by ARO grant (Grant No. W911NF-09-0480), and by DARPA grant (Grant No. N66001-10-1-4063).

## APPENDIX: EXCITATION DYNAMICS

We model the excitation transport by allowing for a perturbative scattering of the excitons on environmental acoustic phonon modes.<sup>22,23,48,59</sup> That is, we consider the exciton-phonon coupling term as a perturbation to the Frenkel exciton Hamiltonian Eq. (1), thus allowing for scattering between exciton states by interaction with phonon modes. We consider a bath that relaxes back to equilibrium on a short timescale compared to the typical exciton dynamics, and assume that the time evolution of the coherences and the populations decou-

ple; formally, this corresponds to making the Born-Markov and secular approximations.<sup>74,75</sup> This leads to a decoupling of the time evolution of exciton populations and exciton coherences, and the populations of the eigenstates  $|s\rangle$  evolve in time according to the Pauli master equation,

$$\dot{P}_s(t) = \sum_{s'} [W_{ss'} P_{s'}(t) - W_{s's} P_s(t)]. \quad (\text{A1})$$

Note that we have neglected radiative decay here, as we want to focus only on the transport. In Sec. III A, we will provide some estimates wherein this assumption is shown to be reasonable for the considered timescales. In Eq. (A1),  $W_{ss'}$  is the scattering rate from state  $s'$  to state  $s$ , given by<sup>22</sup>

$$W_{ss'} = W^{(0)} S(|E_s - E_{s'}|) \sum_{n=1}^N |c_{sn}|^2 |c_{s'n}|^2 \times \begin{cases} n_T(E_s - E_{s'}), & E_s > E_{s'} \\ 1 + n_T(E_{s'} - E_s), & E_s < E_{s'} \end{cases}. \quad (\text{A2})$$

Here, the scattering amplitude  $W^{(0)}$  is a constant that is related to the strength of the exciton-phonon coupling,  $S(E)$  is the phonon spectral density,  $\sum_{n=1}^N |c_{sn}|^2 |c_{s'n}|^2$  is the overlap factor between the initial and final scattering states, and  $n_T(E) = [\exp(E/T) - 1]^{-1}$  describes the thermal occupancy of the phonon modes at temperature  $T$ . For the spectral density  $S(E)$ , we use a Debye-like form with an exponential cut-off factor,  $S(E) = |E/J|^3 \exp(-E/\omega_c)$ , where  $\omega_c$  is the cut-off frequency. Note that generally  $W_{ss'} \neq W_{s's}$ ; in fact, the scattering rates obey the detailed balance condition,

$$W_{s's} = W_{ss'} \exp(E_s - E_{s'})/k_B T \quad (\text{A3})$$

implying that at long times the population distribution thermalizes to a Boltzmann distribution.

We rewrite Pauli master equation (A1) as

$$\dot{P}_s(t) = - \sum_{s'} R_{ss'} P_{s'}(t), \quad (\text{A4})$$

where we have introduced the matrix  $\hat{R}$  given by

$$R_{ss'} = \sum_r W_{rs} \delta_{ss'} - W_{ss'}. \quad (\text{A5})$$

The formal solution of Eq. (A4) reads

$$P_s(t) = \sum_{s'} (e^{-\hat{R}t})_{ss'} P_{s'}(0). \quad (\text{A6})$$

For a given initial state  $P_{s'}(0)$ , this allows us to calculate the exciton populations  $P_s(t)$ . The population of site  $n$ , which we denote by  $p_n(t)$ , is related to  $P_s(t)$  by

$$p_n(t) = \sum_s P_s(t) |c_{sn}|^2. \quad (\text{A7})$$

Once the time evolution of the populations are known, we can consider the corresponding displacement and mean square displacement. Since the transition energies are chosen randomly from the same distribution for all sites (which implies in particular that for all sites the mean energies are identical), there is no net directionality and the displacement vanishes when one averages over realizations.

The mean position  $\langle n(t) \rangle$  of the excitation at time  $t$  is given by a weighted sum

$$\langle n(t) \rangle = \sum_s P_s(t) \langle n \rangle_s, \quad (\text{A8})$$

where the mean position of the excitation in the exciton state  $s$  is given by

$$\langle n \rangle_s = \sum_n n |c_{sn}|^2. \quad (\text{A9})$$

For an excitation that is initially localized on site  $n_0$ , we define the second moment as

$$\langle n^2(t) \rangle = \sum_n p_n(t) (n - n_0)^2 = \sum_n \sum_s P_s(t) |c_{sn}|^2 (n - n_0)^2, \quad (\text{A10})$$

where  $P_s$  is the population of exciton state  $s$ , and  $p_n$  is the population of monomer  $n$  in the site basis.

<sup>1</sup>H. van Amerongen, L. Valkunas, and R. van Grondelle, *Photosynthetic Excitons* (World Scientific, Singapore, 2000).  
<sup>2</sup>V. Sundström, T. Pullerits, and R. van Grondelle, *J. Phys. Chem. B* **103**, 2327 (1999).  
<sup>3</sup>H. Sumi, *J. Phys. Chem. B* **103**, 252 (1999).  
<sup>4</sup>K. Mukai, S. Abe, and H. Sumi, *J. Phys. Chem. B* **103**, 6096 (1999).  
<sup>5</sup>F. C. Spano, *Annu. Rev. Phys. Chem.* **57**, 217 (2006).  
<sup>6</sup>See, e.g., *Semiconducting Polymers – Chemistry, Physics, and Engineering*, edited by G. Hadziioannou and P. van Hutten (VCH, Weinheim, 1999).  
<sup>7</sup>J. C. Bolinger, M. C. Traub, T. Adachi, and P. F. Barbara, *Science* **331**, 565 (2011); C. Bardeen, *ibid.* **331**, 544 (2011).  
<sup>8</sup>K. Colby, J. J. Burdett, R. F. Frisbee, L. Zhu, R. J. Dillon, and C. J. Bardeen, *J. Phys. Chem. A* **114**, 3471 (2010).  
<sup>9</sup>*J-aggregates*, edited by T. Kobayashi (World Scientific, Singapore, 1996).  
<sup>10</sup>T. E. Kaiser, I. G. Scheblykin, D. Thomsson, and F. Würthner, *J. Phys. Chem. B* **113**, 15836 (2009).  
<sup>11</sup>F. Würthner, T. E. Kaiser, and C. R. Saha-Möller, *Angew. Chem., Int. Ed.* **50**, 3376 (2011).  
<sup>12</sup>H. Marciniak, X.-Q. Li, F. Würthner, and S. Lochbrunner, *J. Phys. Chem. A* **115**, 648 (2011).  
<sup>13</sup>S. Valleau, S. K. Saikin, M.-H. Yung, and A. Aspuru-Guzik, *J. Chem. Phys.* **137**, 034109 (2012).  
<sup>14</sup>See contributions to *Quantum Coherence, Correlation, and Decoherence in Semiconductor Nanostructures*, edited by T. Takagahara (Elsevier Science, New York, USA, 2003).  
<sup>15</sup>H. Akiyama, *J. Phys.: Condens. Matter* **10**, 3095 (1998); X.-L. Wang and V. Voliotis, *J. Appl. Phys.* **99**, 121301 (2006).  
<sup>16</sup>G. D. Scholes and G. Rumbles, *Nature Mater.* **5**, 683 (2006).  
<sup>17</sup>J.-L. Brédas, J. E. Norton, J. Cornil, and V. Coropceanu, *Acc. Chem. Res.* **42**, 1691 (2009).  
<sup>18</sup>R. C. Powell and Z. G. Soos, *J. Lumin.* **11**, 1 (1975).  
<sup>19</sup>V. Sundström, T. Gillbro, R. A. Gadonas, and A. Piskarskas, *J. Chem. Phys.* **89**, 2754 (1988).  
<sup>20</sup>M. A. Baldo and S. R. Forrest, *Phys. Rev. B* **62**, 10958 (2000); M. A. Baldo, C. Adachi, and S. R. Forrest, *ibid.* **62**, 10967 (2000).  
<sup>21</sup>I. V. Ryzhov, G. G. Kozlov, V. A. Malyshev, and J. Knoester, *J. Chem. Phys.* **114**, 5322 (2001).  
<sup>22</sup>M. Bednarz, V. A. Malyshev, and J. Knoester, *J. Chem. Phys.* **117**, 6200 (2002); *Phys. Rev. Lett.* **91**, 217401 (2003).  
<sup>23</sup>D. J. Heijs, V. A. Malyshev, and J. Knoester, *Phys. Rev. Lett.* **95**, 177402 (2005).  
<sup>24</sup>R. W. Munn and R. Silbey, *J. Chem. Phys.* **68**, 2439 (1978); *Mol. Cryst. Liq. Cryst.* **57**, 131 (1980); *J. Chem. Phys.* **83**, 1843 (1985); **83**, 1854 (1985).  
<sup>25</sup>R. Silbey and R. W. Munn, *J. Chem. Phys.* **72**, 2763 (1980).  
<sup>26</sup>V. M. Kenkre, *J. Stat. Phys.* **30**, 293 (1983).  
<sup>27</sup>A. V. Malyshev, V. A. Malyshev, and F. Domínguez-Adame, *Chem. Phys. Lett.* **371**, 417 (2003); *J. Phys. Chem. B* **107**, 4418 (2003).  
<sup>28</sup>J. Roden, A. Eisfeld, W. Wolff, and W. T. Strunz, *Phys. Rev. Lett.* **103**, 058301 (2009).

<sup>29</sup>P. W. Anderson, *Phys. Rev.* **109**, 1492 (1958); E. Abrahams, P. W. Anderson, D. C. Licciardello, and T. V. Ramakrishnan, *Phys. Rev. Lett.* **42**, 673 (1979).  
<sup>30</sup>B. Kramer and A. MacKinnon, *Rep. Prog. Phys.* **56**, 1469 (1993).  
<sup>31</sup>J. Roden, W. T. Strunz, K. B. Whaley, and A. Eisfeld, *J. Chem. Phys.* **137**, 204110 (2012).  
<sup>32</sup>J. Müller, D. Haarer, and B. M. Kharlamov, *Phys. Lett. A* **281**, 64 (2001).  
<sup>33</sup>B. M. Kharlamov and G. Zumofen, *J. Chem. Phys.* **116**, 5107 (2002).  
<sup>34</sup>E. Barkai, R. Silbey, and G. Zumofen, *Phys. Rev. Lett.* **84**, 5339 (2000).  
<sup>35</sup>E. Barkai, A. V. Naumov, Yu. G. Vainer, M. Bauer, and L. Kador, *Phys. Rev. Lett.* **91**, 075502 (2003).  
<sup>36</sup>P. Lévy, *Théorie de l'Addition des Variables Aléatoires* (Gautier Villars, Paris, 1954); B. V. Gnedenko and A. N. Kolmogorov, *Limit Distributions for Sums of Independent Random Variables* (Addison-Wesley, Reading, MA, 1954).  
<sup>37</sup>A. Eisfeld, S. M. Vlaming, V. A. Malyshev, and J. Knoester, *Phys. Rev. Lett.* **105**, 137402 (2010).  
<sup>38</sup>R. Metzler and J. Klafter, *Phys. Rep.* **339**, 1 (2000).  
<sup>39</sup>M. F. Shlesinger, G. M. Zaslowski, and J. Klafter, *Nature (London)* **363**, 31 (1993).  
<sup>40</sup>A. Ott, J. P. Bouchaud, D. Langevin, and W. Urbach, *Phys. Rev. Lett.* **65**, 2201 (1990).  
<sup>41</sup>I. M. Sokolov, J. Mai, and A. Blumen, *Phys. Rev. Lett.* **79**, 857 (1997).  
<sup>42</sup>E. Pereira, J. M. G. Martinho, and M. N. Berberan-Santos, *Phys. Rev. Lett.* **93**, 120201 (2004).  
<sup>43</sup>P. Barthelemy, J. Bertolotti, and D. S. Wiersma, *Nature (London)* **453**, 495 (2008).  
<sup>44</sup>A. V. Chechkin, V. Yu. Gonchar, and M. Szydłowski, *Phys. Plasmas* **9**, 78 (2002).  
<sup>45</sup>D. S. Novikov, M. Drndić, L. S. Levitov, M. A. Kastner, M. V. Jarosz, and M. G. Bawendi, *Phys. Rev. B* **72**, 075309 (2005).  
<sup>46</sup>D. S. Novikov, E. Frieremans, J. H. Jensen, and J. A. Halpern, *Nature Phys.* **7**, 508 (2011).  
<sup>47</sup>B. Halperin and M. Lax, *Phys. Rev.* **148**, 722 (1966); I. M. Lifshits, *Zh. Exprim. Theor. Fiz.* **53**, 743 (1967) [*Sov. Phys. JETP* **26**, 462 (1968)]; I. M. Lifshits, S. A. Gredeskul, and L. A. Pastur, *Introduction to the Theory of Disordered Systems* (Wiley, New York, 1988).  
<sup>48</sup>A. S. Davydov, *Theory of Molecular Excitons* (Plenum, New York, 1971).  
<sup>49</sup>V. M. Agranovich and M. D. Galanin, in *Electronic Excitation Energy Transfer in Condensed Matter*, edited by V. M. Agranovich and A. A. Maradudin (North Holland, Amsterdam, 1982); V. Agranovich, *Excitations in Organic Solids* (Oxford University Press, Oxford, 2009).  
<sup>50</sup>*Mathematical Foundations of Quantum Mechanics* (Princeton University Press, Princeton, NJ, 1955).  
<sup>51</sup>M. Schreiber and Y. Toyozawa, *J. Phys. Soc. Jpn.* **51**, 1528 (1982); **51**, 1537 (1982).  
<sup>52</sup>H. Fidler, J. Knoester, and D. A. Wiersma, *J. Chem. Phys.* **95**, 7880 (1991).  
<sup>53</sup>D. J. Thouless, *Phys. Rep., Phys. Lett.* **13**, 93 (1974).  
<sup>54</sup>E. W. Knapp, *Chem. Phys.* **85**, 73 (1984).  
<sup>55</sup>S. M. Vlaming, V. A. Malyshev, and J. Knoester, *Phys. Rev. B* **79**, 205121 (2009).  
<sup>56</sup>A. Eisfeld and J. S. Briggs, *Phys. Rev. Lett.* **96**, 113003 (2006).  
<sup>57</sup>V. Malyshev and P. Moreno, *Phys. Rev. B* **51**, 14587 (1995).  
<sup>58</sup>F. Domínguez-Adame and V. A. Malyshev, *Am. J. Phys.* **72**, 226 (2004).  
<sup>59</sup>S. M. Vlaming, V. A. Malyshev, and J. Knoester, *J. Chem. Phys.* **127**, 154719 (2007).  
<sup>60</sup>N. G. van Kampen, *Stochastic Processes in Physics and Chemistry* (North-Holland, Amsterdam, 1981).  
<sup>61</sup>J.-P. Bouchaud and A. Georges, *Phys. Rep.* **195**, 127 (1990).  
<sup>62</sup>B. D. Hughes, *Random Walks and Random Environments, Vol. 1: Random Walks* (Oxford University Press, Oxford, 1995).  
<sup>63</sup>A. V. Malyshev and V. A. Malyshev, *Phys. Rev. B* **63**, 195111 (2001).  
<sup>64</sup>H. Fidler, J. Knoester, and D. A. Wiersma, *Chem. Phys. Lett.* **171**, 529 (1990).  
<sup>65</sup>I. Renge and U. P. Wild, *J. Phys. Chem. A* **101**, 7977 (1997).  
<sup>66</sup>A. Eisfeld and J. S. Briggs, *Chem. Phys.* **324**, 376 (2006).  
<sup>67</sup>S. de Boer and D. A. Wiersma, *Chem. Phys. Lett.* **165**, 45 (1990).  
<sup>68</sup>V. F. Kamalov, I. A. Struganova, and K. Yoshihara, *J. Phys. Chem.* **100**, 8640 (1996).  
<sup>69</sup>I. G. Scheblykin, O. Yu. Sliusarenko, L. S. Lepnev, A. G. Vitukhnovsky, and M. Van der Auweraer, *J. Phys. Chem. B* **105**, 4636 (2001).

- <sup>70</sup>J. Klafter and R. Silbey, *J. Chem. Phys.* **72**, 843 (1980); **72**, 849 (1980).
- <sup>71</sup>J. Bernasconi, S. Alexander, and R. Orbach, *Phys. Rev. Lett.* **41**, 185 (1978); J. Bernasconi, W. R. Schneider, and W. Wyss, *Z. Phys. B* **37**, 175 (1980).
- <sup>72</sup>H. Scher and E. W. Montroll, *Phys. Rev. B* **12**, 2455 (1975).
- <sup>73</sup>J. Nolan, *Stable Distributions: Models for Heavy-Tailed Data* (Birkhäuser, 2003).
- <sup>74</sup>K. Blum, *Density Matrix Theory and Applications* (Plenum, New York, 1981).
- <sup>75</sup>V. May and O. Kühn, *Charge and Energy Transfer Dynamics in Molecular Systems* (Wiley-VCH, Berlin, 2000).